A Study of Tsunami Wave Fission in an Undistorted Experiment

4 authors:

Masafumi Matsuyama
Central Research Institute of Electric Power Industry
83 PUBLICATIONS   617 CITATIONS

SEE PROFILE

Masaaki Ikeno
Central Research Institute of Electric Power Industry
23 PUBLICATIONS   67 CITATIONS

SEE PROFILE

Tsutomu Sakakiyama
Central Research Institute of Electric Power Industry
19 PUBLICATIONS   909 CITATIONS

SEE PROFILE

Tomoyoshi Takeda
Tokyo Electric Power Company
8 PUBLICATIONS   63 CITATIONS

SEE PROFILE

A Study of Tsunami Wave Fission in an Undistorted Experiment

MASAFUMI MATSUYAMA,[1] MASAAKI IKENO,[1]
TSUTOMU SAKAKIYAMA,[1] and TOMOYOSHI TAKEDA[2]

Abstract—To study tsunami soliton fission and split wave-breaking, an undistorted experiment was carried out which investigated tsunami shoaling on a continental shelf. Three models of the continental shelf were set up in a 205-m long 2-dimensional flume. Each shelf model was 100 m, long with slopes of either 1/100, 1/150, or 1/200. Water surface elevations were measured across the flume, including a dense cluster of wave gages installed around the point of wave-breaking. We propose new methods for calculating wave velocity and the wave-breaking criterion based on our interpretation of time series data of water surface elevation. At the point of wave-breaking, the maximum slope of water surface is between 20 to 50 deg., while the ratio of surface water particle horizontal velocity to wave velocity is from 0.5 to 1.2. The values determined by our study are larger than what has been reported by other researchers.

Key words: Tsunami, shoaling, soliton fission, wave-breaking, an undistorted experiment.

1. Introduction

On May 26 in 1983, an earthquake of magnitude 7.7 occurred in the Japan Sea, generating a large tsunami, known as the 1983 Nihonkai-Chubu earthquake tsunami. During that event, 'tsunami soliton fission' was observed on the gentle seabed slope in the shallow water along the coast (SHUTO, 1985). This phenomena occurs when short waves split from the tsunami crest due to nonlinearity and dispersion. When soliton fission occurs, the new leading wave height increases and breaks. It is therefore important to investigate the characteristics relative to breaking of tsunami soliton fission.

SHAFFER *et al.* (1993) and MADSEN *et al.* (1997) used the local slope (θ) of a wave profile as a breaking criteria for wind waves. SHAFFER *et al.* (1993) found that acceptable results could be obtained by using the value $\theta_b = 20$ deg. for spilling breakers, and $\theta_b = 25$ deg. for plunging breakers.

SATO (1996) and IWASE *et al.* (2004) used the parameter (u_s/c) as a breaking criteria. This number relates the ratio of surface water particle horizontal velocity u_s

[1] Central Research Institute of Electric Power Industry, Japan.
[2] Tokyo Electric Power Company, Tokyo, Japan.

to wave velocity c. SATO (1996) defined a breaker limit $u_s/c = 0.4$ based on experiments for wind waves in the surf zone. SATO (1996) carried out a numerical simulation of 1993 Southwest Hokkaido tsunami and was able to reproduce tsunami soliton fission offshore of Aonae Cape on Okushiri Island by using a finite-difference method based on Boussinesq-type equations with wave-breaking term. In this study he let $c = \sqrt{g(h + \eta)}$ where g is gravitational constant, h is water depth, and η is water surface elevation.

IWASE *et al.* (2004) carried out experiments investigating wave soliton fission on a flat bottom to develop a wave-breaking model. By using the velocity of a stable solitary wave he proposed a breaker limit $u_s/c = 0.59$. These breaking criteria however were not based on a long wave such as a tsunami. In this study the breaking criteria is investigated by simulating tsunami shoaling across a continental in an undistorted model in a two-dimensional flume.

2. Hydraulic Model Experiment

2.1. Flume and Model

The Large Wave Flume located at Central Research Institute of Electric Power Industry, Japan (CRIEPI) is shown in Figure 1. The dimensions are 205 m long, 3.4 m wide, and 6 m deep in the 115 m-long generator-side flat section. The wave generator is the piston type blade, with a maximum stroke of 2.2 m. Three different types of continental shelf models were set up in the flume at an undistorted 1/200 scale. Each model had a different seabed slope, 1/200, 1/150, and 1/100, as shown in Figure 2.
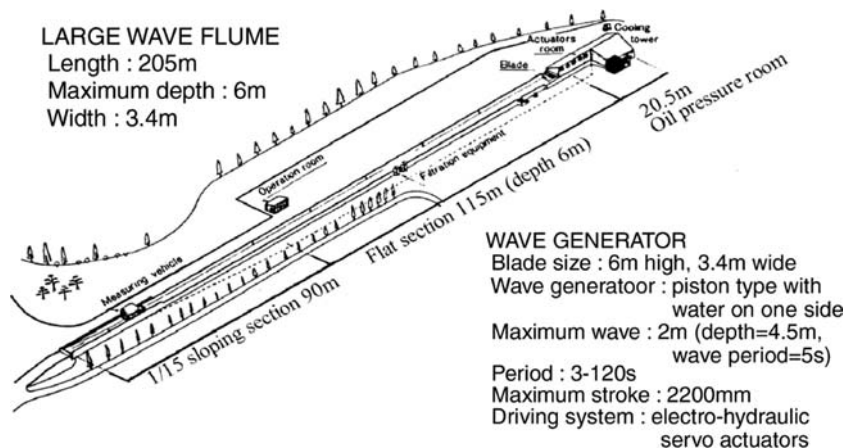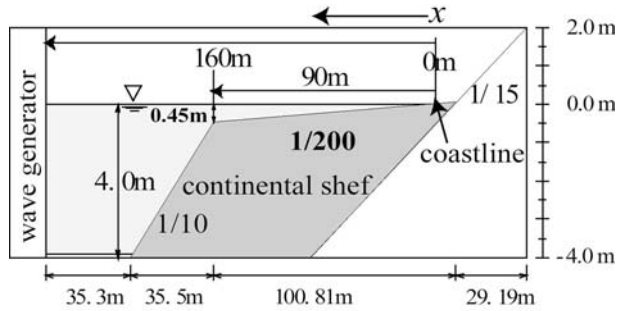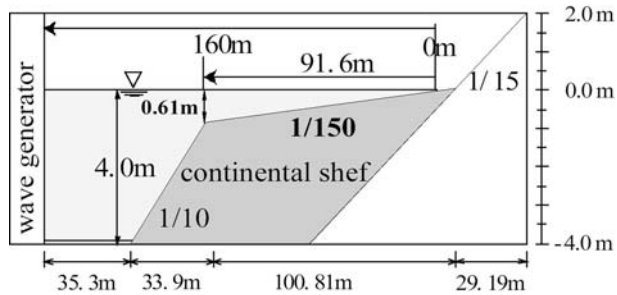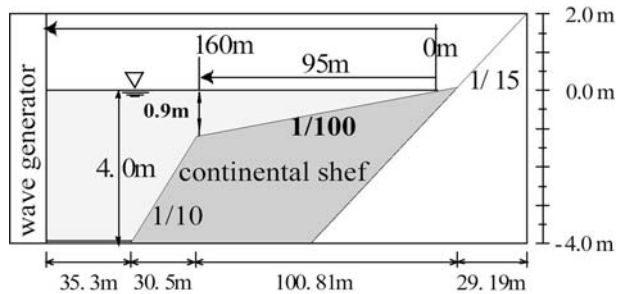

Figure 1
The CRIEPI Large Wave Flume.

Figure 2
Three models of the continental shelf in the wave flume.

2.2. Data Acquisition System

Water surface elevations were measured by capacitance-type wave gages. Ten gages were arranged across the model at intervals of 5, 10, or 20 m (Fig. 3). We first checked where wave-breaking appeared for each wave condition. Ten more gages were then set up at the breaking point with either a 20 or 40 cm interval to resolve the
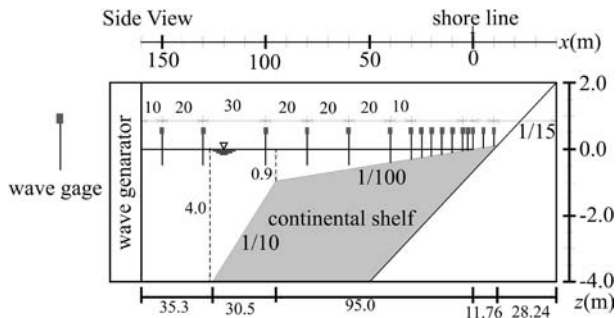
Figure 3

An example of the arrangement of fixed wave gages on the slope 1/100.

wave shape around the breaking point. Water surface elevation was recorded at a time interval of 0.01 sec (100 Hz).

2.3. Incident Wave Condition

Table 1 lists the input wave cases. Input wave profile η_I is a sinusoidal wave shape of only one cycle as shown in Figure 4.

$$
\begin{aligned}
\eta_I &= A \sin\left(\frac{2\pi}{T}t\right) \quad 0 \le t \le T \\
&= 0 \quad t > T
\end{aligned}
, \tag{1}
$$

Table 1

Incident wave condition

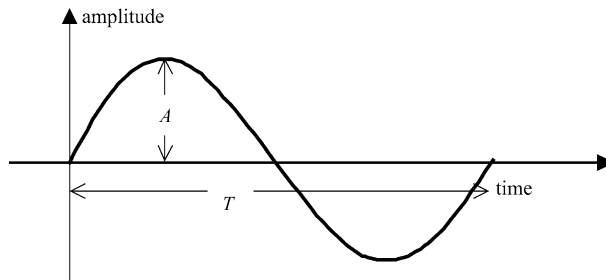| No.	Period(sec)	Amplitude(m)
021	20	0.005
022		0.01
023		0.02
024		0.03
041	40	0.01
042		0.02
043		0.03
044		0.04
045		0.09
061	60	0.005
062		0.01
063		0.02
064		0.03
065		0.04
121	120	0.01
122		0.02

Figure 4
Incident wave shape.

where η_I is water surface elevation, A is wave amplitude, T is period, and t is time. Input waves ranged in amplitude and period from 0.005 m to 0.09 m and from 20 sec to 120 sec (Table 1). In actual scale, wave periods ranged from 282 s (4.7 min) to 1690 s (28.3 min), which is long enough to reproduce tsunami shoaling on the continental shelf.

Since the aim of this experiment is to keep track of split wave deformation at wave-breaking point and because wave-breaking is a sensitive phenomena, each experimental test was carried out two or more times for each incident wave condition to check for consistency and repeatability.

3. Experimental Results

3.1. Outline of Wave Shoaling

Figure 5 shows time histories of water surface elevation for Case 024 ($T = 20$ sec, $A = 0.03$ m, slope $= 1/200$). Wave height increased and wavelength decreased during propagation across the continental shelf. The soliton fission was observed as a split wave with new short waves appearing. Three short waves appeared with approximately 1 second between subsequent crests. These short waves amplified remarkably just before breaking. The new wave height at the point of breaking is about 0.14 m, which is twice as big as the wave height at the beginning of soliton fission. As shown in Photo 1, plunging breakers were produced. After wave-breaking, the height of the split wave decreased through energy dissipation. When converted to actual scale, the period of short waves is approximately 14 sec., which is similar to observations of wave fission during the 1983 Nihonkai-Chubu Earthquake Tsunami (SHUTO, 1985).

Figure 6 shows the time histories of water surface elevation for Case 063 ($T = 60$ sec, $A = 0.02$ m, slope $= 1/200$). In this case, a new wave crest is not observed at the tsunami peak, but rather on the wavefront. That is, wave split point has moved forward relative to the tsunami crest. The tendency increased in frequency, as the period of incident wave exists longer.
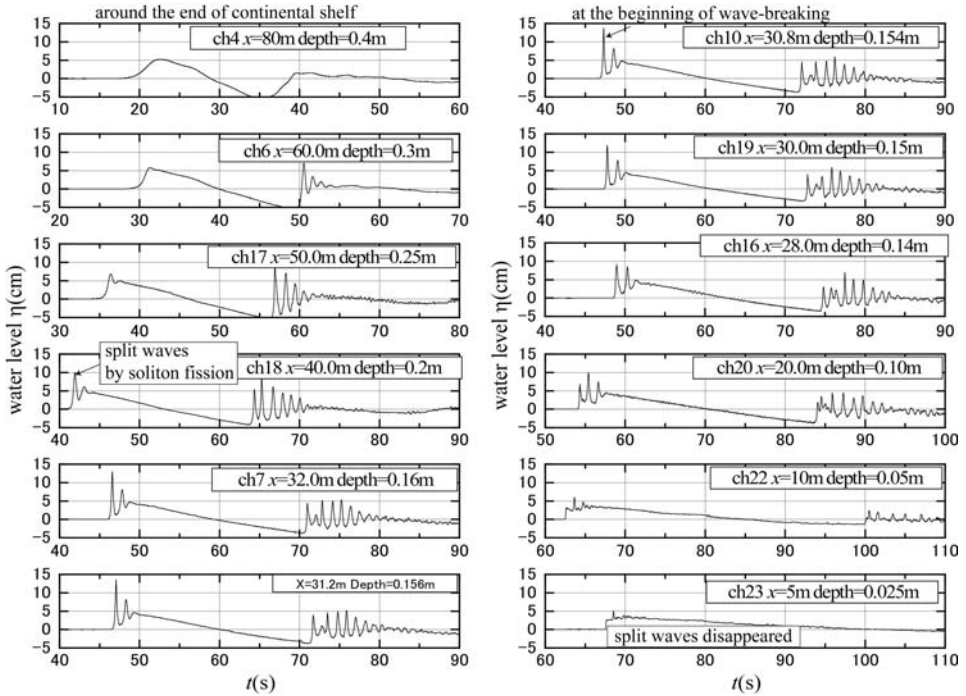
Figure 5
Time histories of water surface elevation for Case 024 ($T = 20$ sec., $A = 0.03$ m, slope $= 1/200$).

3.2. Wave-breaking

3.2.1. Breaking wave height and water depth

Figure 7 shows the time histories of water surface elevation at the moment of wave-breaking for two different incident wave conditions on seabed slopes of 1/100, 1/150, and 1/200. These figures show differences in wave shape and deformation at wave-breaking for different seabed slopes. For Case 024, the breaking height for the first split wave is 0.144 m on 1/200 slope, 0.148 m on 1/150 slope, and 0.142 m on 1/100 slope. For Case 063 the values are 0.064 m on 1/200, 0.061 m on 1/150, and 0.053 m on 1/100. Thus, breaking-wave heights on three slopes are comparable. On the other hand, as seabed slope increases, the water depth at breaking is smaller, i.e., 0.150 m on 1/200, 0.148 m on 1/150, and 0.128 m on 1/100 for Case 024. As a result, ε_b, which is the ratio of maximum wave surface level η of the first split wave to water depth h at the wave-breaking point, is larger, as the seabed slope increases. Figure 8 shows ε_b for all plotted against water depth at wave-breaking. The range of ε_b was from 0.7 to 1.4. Average values of ε_b with respect to each seabed slope are 0.87 for 1/200, 1.00 for 1/150, and 1.23 for 1/100.
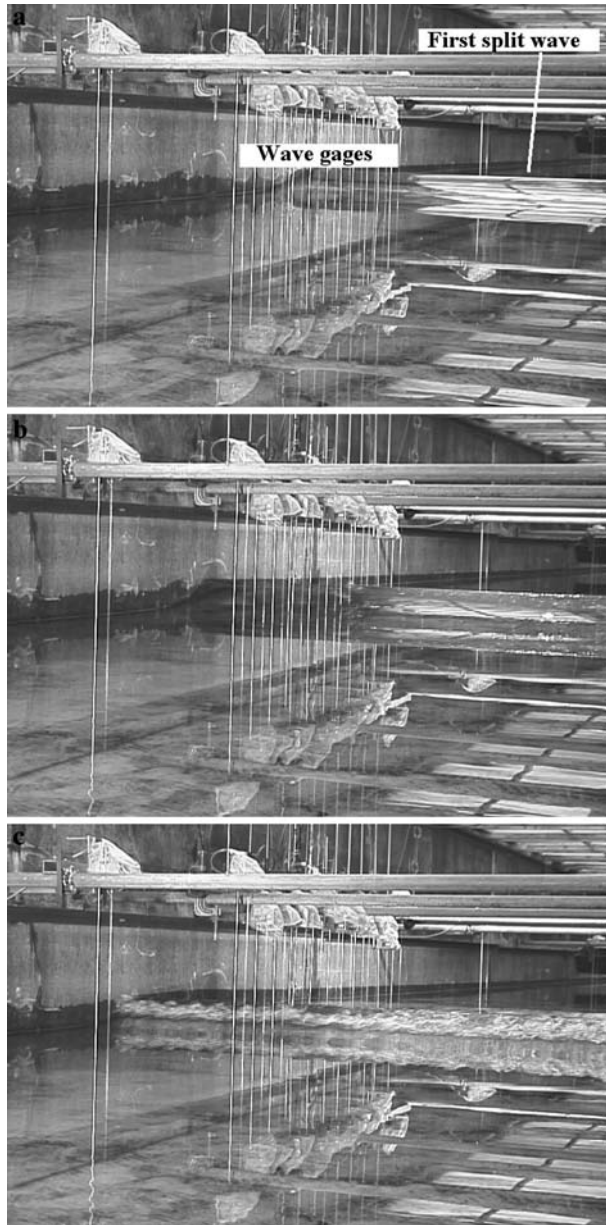
Photo 1
Snapshots around the break point for Case No. 024. (a) Before wave-breaking, (b) At wave-breaking, (c) After wave-breaking.
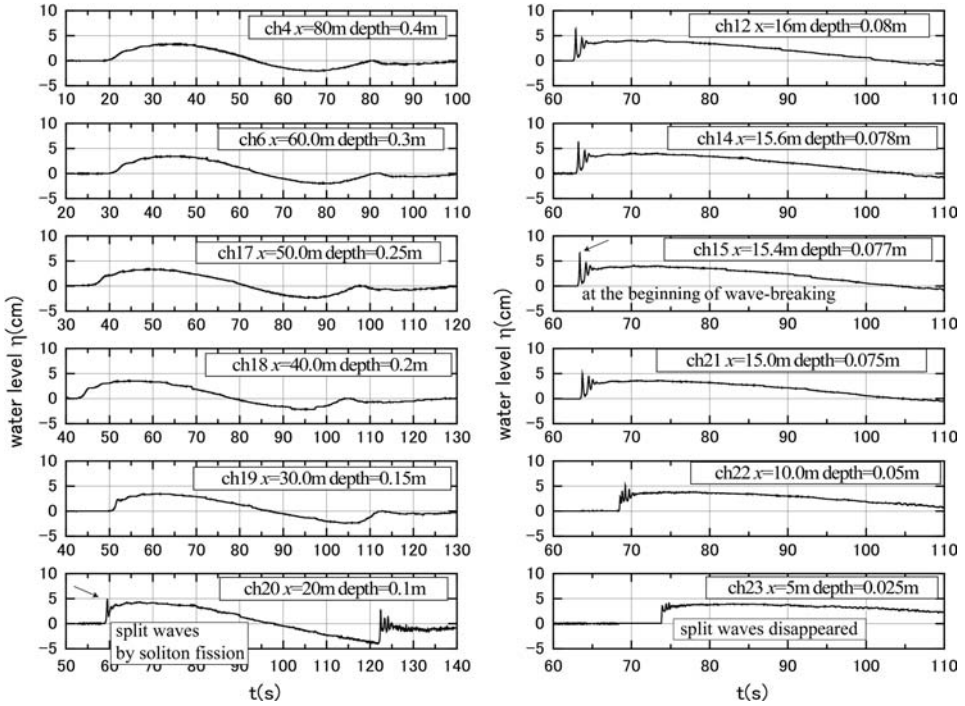
Figure 6
Time histories of water surface elevation for Case 063 ($T = 60$ sec., $A = 0.02$ m, slope $= 1/200$).

3.2.2. Breaking criterion

Two parameters related to the breaking criterion were investigated. One is local slope θ of the water surface and the other is the ratio of water surface particle velocity u_s to wave horizontal velocity c (u_s/c).

(1) Wave velocity

Wave velocity c is necessary to convert time histories of water surface elevation to spatial wave shape. Thus a new method is proposed, which is based on nonlinear dispersion wave theory. For shallow water waves with dispersion over gentle slope, one-dimensional Boussinesq equation is expressed as

$$\frac{\partial \eta}{\partial t} + \frac{\partial M}{\partial x} = 0 \tag{2}$$

$$\frac{\partial M}{\partial t} + \frac{\partial}{\partial x}\left(\frac{M^2}{D}\right) + gD\frac{\partial \eta}{\partial x} = \frac{1}{3}h^3\frac{\partial^3 \bar{u}}{\partial t \partial x^2}, \tag{3}$$

where M is flux, h is still water depth, D is $\eta + h$, $\bar{u}$ is horizontal velocity averaged vertically. Assumed wave profile is not deformed in small time Δt, progressive wave velocity c is defined as follows:
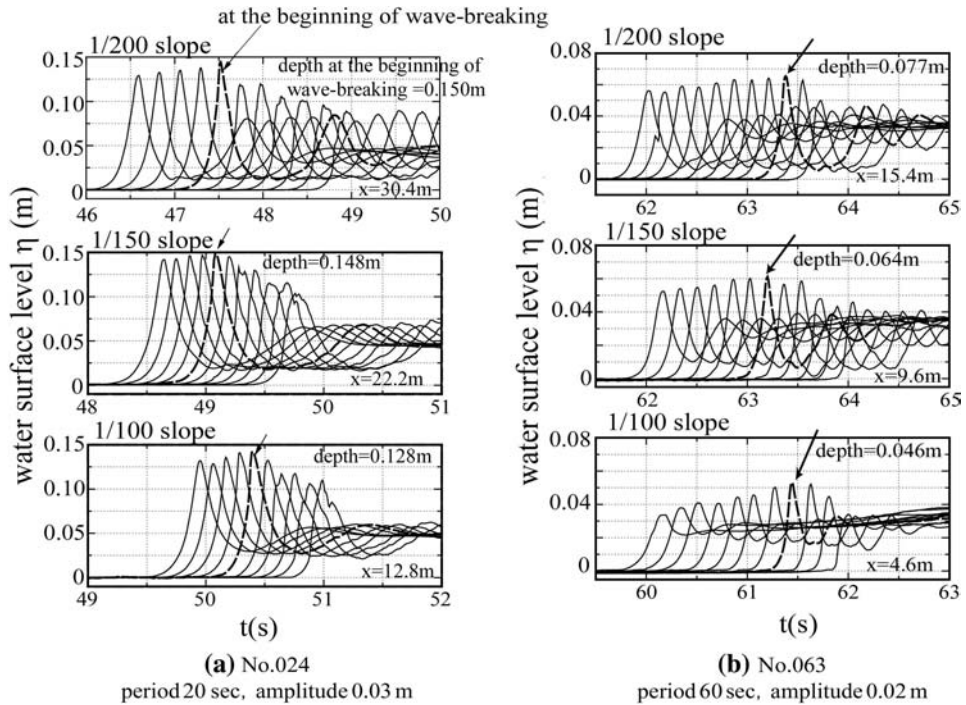
Figure 7
Time histories of the first split wave at the wave-breaking point.

$$\frac{\partial}{\partial t} = -c\frac{\partial}{\partial x}. \tag{4}$$

Equations (2) and (4) are combined to give

$$M = c\eta. \tag{5}$$

Equations (4) and (5) to (3) reduced to

$$c\eta - \frac{c\eta^2}{D} - \frac{gD}{c}\eta - \frac{1}{3}\frac{h^3}{c}\left[\frac{1}{(h+\eta)^3}\left\{h(h+\eta)\frac{\partial^2\eta}{\partial t^2} - 2h\left(\frac{\partial\eta}{\partial t}\right)^2\right\}\right] = 0. \tag{6}$$

Wave velocity c can be evaluated by using time series data of water surface elevation accordingly, as follows:

$$c_t = \sqrt{gh}\sqrt{(1+\varepsilon)^2 + \frac{1}{3gh\varepsilon(1+\varepsilon)^2}\left\{D\frac{\partial^2\eta}{\partial t^2} - 2\left(\frac{\partial\eta}{\partial t}\right)^2\right\}}, \tag{7}$$

where $\varepsilon = \eta/h$.

　　Figure 9 shows the wave profile and a ratio of wave velocity c_t by equation (7) to c_p, which is calculated by phase delay based on a time lag between wave crests of
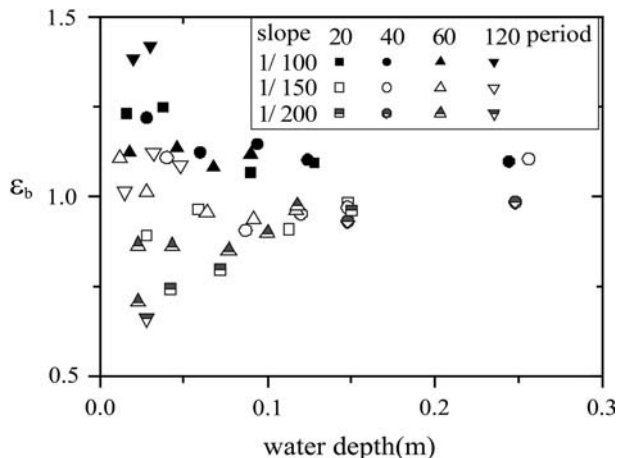
Figure 8
$\varepsilon_b(\eta/h)$ versus water depth at the wave-breaking point.

adjacent wave gages. The ratio is almost 1.0 except for both edges of the split wave. This result indicates the adequacy of equation (7) at least for progressive waves.

(2) Local slope θ of water elevation

The local slope of water surface θ, is obtained from time series data for η and wave velocity c by the following equation.

$$\theta = \tan^{-1}\left(-\frac{1}{c_t}\frac{\partial\eta}{\partial t}\right). \tag{8}$$

Figure 10 shows time histories of water surface elevation η and local slope θ at the wave-breaking point for the first split wave on the 1/100 slope. In each case, wave-breaking began when θ exceeded 30°.

Figure 11 shows the maximum local slope $\theta(=\theta_b)$ at the breaking point for all cases. θ_b ranges from 20 to 50 deg., and increases with wave velocity. As shown in Photo 1, the waves are breaking in a plunging fashion. According to Figure 11, the breaker limit seems to be at $\theta_b = 30$ deg. for plunging breakers. We assumed that for cases θ_b is more than 30 deg., wave-breaking has already begun and the wave is beginning to lose shape. Bottom slope is not related to breaker limit θ_b.

(3) Ratio of surface water particle horizontal velocity to wave velocity u_s/c

FUJIMA *et al.* (1986) examined the accuracy of nonlinear dispersive long-wave equations by higher order approximation. They derived an equation for u_s under the condition of $\varepsilon \sim 1$ and $\sigma \gg 1$ ($\sigma = (L/h)^2$). When the bottom slope is gentle, the equation is expressed as below.

(a) Case.024: $T = 20$ sec, $A = 0.03$ m, slope $= 1/100$

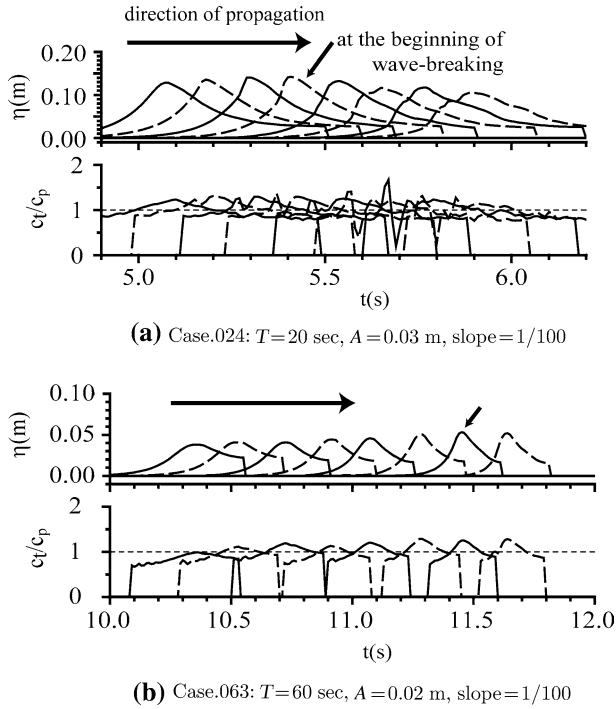**(b)** Case.063: $T = 60$ sec, $A = 0.02$ m, slope $= 1/100$

Figure 9
Wave profile, ratio c_t/c_p around the point of wave-breaking.

$$u_S = \bar{u} - \frac{D^2}{3}\frac{\partial^2 \bar{u}}{\partial x^2}. \tag{9}$$

If equations (4) and (5) are applied to equation (9), we obtain equations of u_s/c for the progressive wave.

$$\frac{u_S}{c} = \frac{\eta}{D} - \frac{h}{3D}\left\{D\frac{\partial^2 \eta}{\partial x^2} - 2\left(\frac{\partial \eta}{\partial x}\right)^2\right\} \tag{10}$$

and

$$\frac{u_S}{c} = \frac{\eta}{D} - \frac{h}{3Dc^2}\left\{D\frac{\partial^2 \eta}{\partial t^2} - 2\left(\frac{\partial \eta}{\partial t}\right)^2\right\}, \tag{11}$$

where D is $\eta + h$. In equation (10) the values of u_s/c are expressed by wave shape and water depth h. On the other, u_s/c is expressed by time histories of water surface elevation, wave velocity c, and water depth h in equation (11). According to equations (7) and (11) we are able to estimate the values of u_s/c from time histories data of water surface elevation η and water depth h.
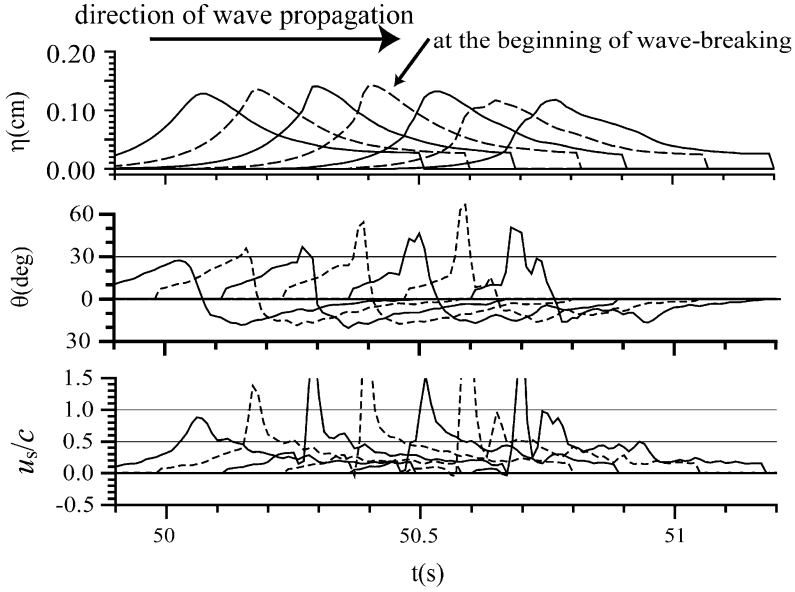
(a) Case.024: $T = 20$ sec, $A = 0.03$ m, slope$= 1/100$
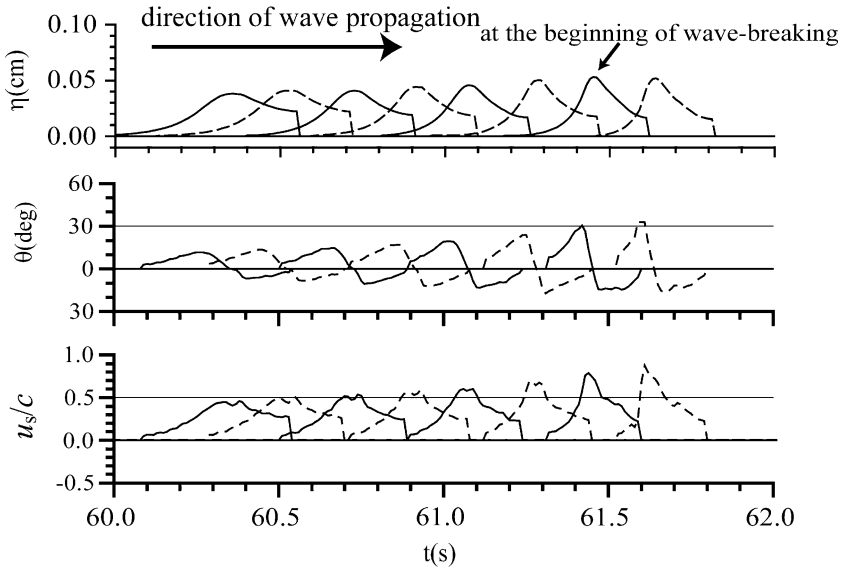
(b) Case.063: $T = 60$ sec, $A = 0.02$ m, slope$= 1/100$

Figure 10

Time histories for water surface elevation and parameters θ and u_s/c near the wave-breaking point for the first split wave.
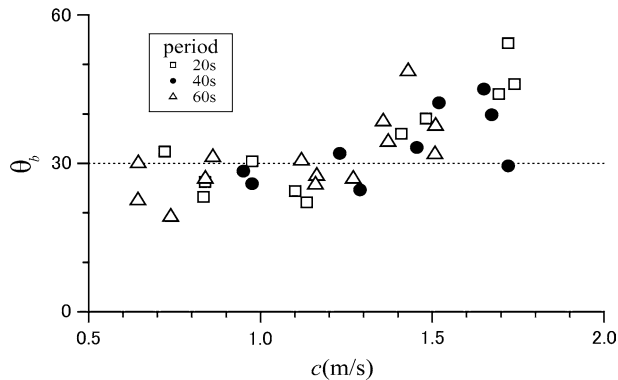
Figure 11
The maximum slope θ_b of water surface elevation at the point of wave-breaking.

Figure 10 shows time histories of η and u_s/c around the wave-breaking point for cases 024 and 063. The maximum value for u_s/c was not observed at the wave crest, but rather at a point slightly ahead of the crest in both cases. Peak values of u_s/c at peak increased toward the wave-breaking point. u_s/c exceeded 1.5 for Case 024 and reached 0.8 for Case 063.

Figure 12 shows γ, which is maximum u_s/c at the wave-breaking point. This value generally ranges between 0.5 to 1.2 except for a few cases and increases with wave velocity. We therefore suggest that the wave-breaking limit u_s/c should be set to 0.9 so as not to underestimate the maximum wave height and wave force. The values for λ determined here are larger than values reported in previous studies, i.e., $\gamma = 0.59$ in IWASE et al. (2004).

Differences in model bathymetry may explain the discrepancy between the two studies. IWASE (2004) experiments used considerably steeper slopes which resulted in less stable split waves than in the present experiment, resulting in a smaller value for γ.

4. Conclusions and Future Work

An undistorted experiment was carried out to study tsunami soliton fission and split wave-breaking. We obtained time series data of water surface elevations around the wave-breaking point after tsunami shoaling and soliton fission on a continental shelf.

The major conclusions of the present study can be summarized as follows:
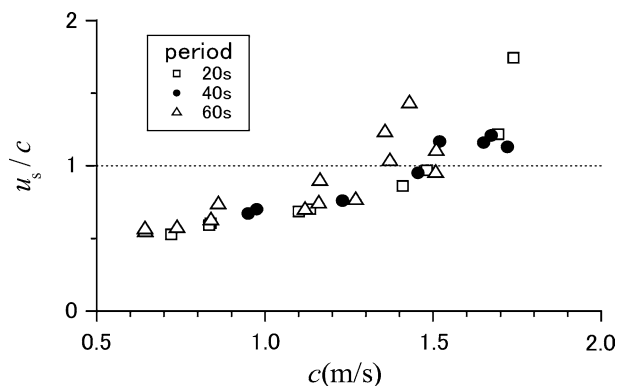1) The wave split point has moved forward to the tsunami crest, as the period of incident wave is longer.

Figure 12
Values for u_s/c at the point of wave-breaking.

2) Wave height of split waves at breaking is not related to the bottom slope on a continental shelf. On the other hand, as the bottom slope increases, the water depth h at wave-breaking is smaller and consequently η/h of the first split wave at wave-breaking is larger.

3) We proposed new methods, which are based on a nonlinear dispersion wave theory, to estimate wave velocity and wave-breaking criterion for a progressive wave. Then its capability was demonstrated by applying it to experiment results.

4) λ, which is the maximum u_s/c of split waves at wave-breaking, ranges 0.5 to 1.2 on a continental shelf. The values are larger than values reported in previous studies.

The next step is to integrate the results from this study into numerical models for wave-breaking.

Acknowledgements

REFERENCES

FUJIMA, K., GOTO, T., and SHUTO, N. (1986), *Accuracy of nonlinear dispersive long-wave equations*, J. Japan Society of Civil Engineers, JSCE *369*, II-5, 223–232 (in Japanese).

IWASE, H. and IMAMURA, F. (2004), *A new tsunami numerical simulation with Boussinesq-Type equations applied for the 1983 Nihonka-Chubu Earthquake tsunami*, Proc. APAC2003 Makuhari, Japan, pp. 12–13.

MADSEN, P.A., SØRENSEN, O.R., and SCHÄFFER, H.A. (1997), *Surf zone dynamics simulated by a Boussinesq type model. Part I: Model description and cross-shore motion of regular waves.* Coastal Engin. *32,* 255–287.

SHÄFFER, H.A., MADSEN, P.A., and DEIGAARD, R. (1993), *A Boussinesq model for waves breaking in shallow water*, Coastal Engin. *20*, 185–202.

SATO, S. (1996), *Numerical simulation of 1993 Southwest Hokkaido earthquake tsunami around Okushiri Island*, J. Waterway, Port, Coastal, and Ocean Engin. ASCE, *122*(5), 209–215.

SHUTO, N (1985), *The Nihonkai-Chuubu earthquake tsunami on the north Akita coast*, Coastal Engin. Japan, JSCE *28*, Tokyo, Japan, 255–264.

To access this journal online:
http://www.birkhauser.ch